Structure, Dispersibility, and Crystallinity of Poly(hydroxybutyrate)/Poly(L-lactic acid) Blends Studied by FT-IR Microspectroscopy and Differential Scanning Calorimetry

Tsuyoshi Furukawa,[†,‡] Harumi Sato,[†] Rumi Murakami,[†] Jianming Zhang,[†] Yong-Xin Duan,[†,§] Isao Noda,[⊥] Shukichi Ochiai,[‡] and Yukihiro Ozaki*[,†]

School of Science and Technology and Research Center for Environment Friendly Polymers, Kwansei Gakuin University, Gakuen, Sanda, Hyogo 669-1337, Japan; S.T. Japan Inc. 1-16-27, Minaminakaburi, Hirakata, Osaka 573-0094, Japan; Institute of Chemistry, Chinese Academy of Sciences, Beijing, China; and The Procter & Gamble Company, 8611 Beckett Road, West Chester, Ohio 45069

Received March 5, 2005; Revised Manuscript Received May 22, 2005

ABSTRACT: The present study is aimed at investigating structure, dispersibility, and crystallinity of poly(3-hydroxybutyrate) (PHB) and poly(L-lactic acid) (PLLA) blends by using FT-IR microspectroscopy and differential scanning calorimetry (DSC). Four kinds of PHB/PLLA blends with a PLLA content of 20, 40, 60, and 80 wt % were prepared from chloroform solutions. Micro-IR spectra obtained at different positions of a PHB film are all very similar to each other, suggesting that there is no discernible segregated amorphous and crystalline parts on the PHB film at the resolution scale of micro-IR spectroscopy. On the other hand, the micro-IR spectra of two different positions of a PLLA film, where spherulite structures are observed and they are not observed, are significantly different from each other. PHB and PLLA have characteristic IR marker bands for their crystalline and amorphous components. Therefore, it is possible to explore the structure of each component in the PHB/PLLA blends by using micro-IR spectroscopy. The IR spectra of a position of blends except for the 20/80 blend are similar to that of pure PHB. On the other hand, the IR spectra of another position of the blend consist of the overlap of those of pure PHB and PLLA. For the 20/80 blend, it is difficult to find a position whose spectrum is similar to that of pure PHB. However, a crystalline peak due to the C=O stretching band is observed at 1718 cm^{-1}. This means that PHB crystallizes as very small spherulites or immature spherulites under such blend ratio. DSC curves of the blend show that the heat of crystallization of PHB varies with the blending ratio of PHB and PLLA. The recrystallization peak is detected for PLLA and the 20/80 blend respectively at 106.5 and 88.2 °C. The lowering of recrystallization temperature for the 20/80 blend compared with that of pure PLLA suggests that PHB forms small finely dispersed crystals that may act as nucleation sites of PLLA. The results for the PHB/PLLA blends obtained from IR microspectroscopy indicate that PHB crystallizes in any blends. However, crystalline structures of PHB in the 80/20, 60/40, and 40/60 blends are different from those of the 20/80 blend.

Introduction

Poly(3-hydroxyalkanoate)s (PHAs) are biologically synthesized polyesters produced by microorganisms and are consequently subjected to biodegradation by bacteria in the soil.[1−8] Among PHA polymers, poly(3-hydroxybutyrate) (PHB) is one of the most well-studied bacterial polyesters. The chemical structure and physical properties of PHB are fairly similar to those of certain petroleum-based synthetic polymers. Therefore, PHB has been a matter of extensive studies as an environment-friendly polymeric material. However, the high crystallinity of PHB makes it rigid and stiff, and thus PHB is not necessarily well-suited for certain applications as a commodity plastic. To reduce the excess crystallinity and improve the overall physical properties of PHB, copolymers and blends of PHB have also been investigated.[9−16] PHB has been blended with nonbiodegradable polymers as well as biodegradable polymers. For example, Marthscelli et al.[13,14] investigated thermal and crystallization behavior of PHB blended with poly(ethylene oxide) (PEO), ethylene−propylene rubber (EPR), and poly(vinyl acetate) (PVAc). They also studied radial growth rate of PHB spherulites in the blend. PHB/PEO blends and PHB/PVAc blends are miscible because both blends show single glass transition temperature, a depression of the melting temperature, and the radial growth rate of PHB spherulite. PHB/EPR blends are deemed immiscible because the radial growth rate of PHB in the blend is independent of the EPR content. Azuma et al.[15] analyzed the thermal behavior and miscibility of PHB blends with biodegradable synthetic polymer, poly(vinyl alcohol) (PVA). Their results indicated that melting temperatures of PHB and PVA in the blend are lower than those found for pure PHB and PVA. The melt temperature remains almost unchanged as the PVA content increases, and the miscibility of the blend is enhanced with the increase in the PVA content. Gassner and Owen[16] explored the physical properties and morphologies of PHB blended with poly(ϵ-caprolactone) (PCL).[16] Melting points of both components in the blend shift to lower temperatures depending on the blending ratio, and their structures also have different layered appearances depending on the blending ratio.

Poly(L-lactic acid) (PLLA) is one of the chemically synthesized polyesters.[8,17−19] It can be readily degraded by hydrolysis under mild conditions to lactic acid, which

* Corresponding author: e-mail ozaki@kwansei.ac.jp.
† Kwansei Gakuin University.
‡ S.T. Japan.
§ Chinese Academy of Sciences.
⊥ Procter & Gamble.

10.1021/ma0504668 CCC: $30.25
Published on Web 06/29/2005

is a common biodegradable organic acid naturally present even in the human body. Therefore, PLLA is also a very important environment-friendly polymeric material. PLLA is superior to many other biodegradable polyesters in terms of thermal and mechanical properties and transparency of the processed materials. Therefore, PLLA is used in biomedical applications, such as surgical sutures and implants,[20] drug delivery systems,[21,22] and bone fixation.[23] PLLA is also blended with other polymers. Baer et al.[24−26] investigated the crystallization and morphology of blends comprising PLLA with different stereoregularity and poly(ethylene glycol) (PEG). PLLA/PEG blends have lower modulus and increased fracture strain compared to those of pure PLLA. The amorphous part of the blend with 30 wt % PEG is separated into a rigid PLLA-rich region and a less rigid PEG-rich. The stereoregularity of PLLA significantly affects the miscibility of PLLA/PEG blends. PLLA is also blended with starch, and the thermal and mechanical properties of such blends have been investigated. The additives, like talc and methylenediphenyl diisocyanate, are known to enhance the mechanical properties and increase the crystallization rate of PLLA.[27,28]

The miscibility and crystallinity of binary blends of PHB and PLLA have been investigated.[29−32] The miscibility of PHB/PLLA blends depends on the molecular weight of PHB, and the crystallinity and growth rate of spherulite of PLLA are related with the addition of the low molecular weight PHB component.[29,31] Zhang et al.[32] analyzed the miscibility, crystallization, and morphology of PHB/PLLA blends by using polarized light microscopy, differential scanning calorimetry (DSC), and scanning electron microscopy (SEM) and indicated that the blend properties are affected by the blending ratio of PHB/PLLA.

The purpose of the present study is to investigate the structure, dispersibility, and crystallinity of environment-friendly polymers. PHB, PLLA, and their blends are investigated by using Fourier transform infrared (FT-IR) microspectroscopy and DSC. DSC gives information about thermal properties such as crystallization temperature, melting point, glass transition temperature, and so on.[32−34] IR spectroscopy enables one to explore the structure and interaction of molecules at the functional group level. Therefore, IR spectroscopy has extensively been used to elucidate the crystalline and amorphous structures of polymers.[34−40]

We have investigated the structure and thermal behavior of PHB and its copolymer poly(hydroxybutylate-*co*-hydroxyhexanoate) (PHB-*co*-HHx) (HHx = 2.5, 3.4, and 12 mol %) by using IR spectroscopy and wide-angle X-ray diffraction.[41,42] We found that there is an inter- and intramolecular C−H···O hydrogen bond between the C=O group and the CH_3 group in PHB and P(HB-*co*-HHx). It is very likely that a chain of the C−H···O hydrogen bond pair links two parallel helical structures in the crystalline parts. The weakening of the C−H···O hydrogen bonds starts from just above room temperature, leading to the deformation of helical structures. We also explored the thermal behavior and intermolecular interactions of the poly(L-lactide) (PLLA) and poly(L-lactide)/poly(D-lactide) (PLLA/PDLA) stereocomplex by using IR spectroscopy.[43,44] It has been revealed that PLLA, PLLA/PDLA stereocomplex, and PHB have quite different C−H···O interactions.[44]

In the case of polymer blends such as PHB/PLLA blends, the structure, distribution, and crystallinity of each blend component must be investigated separately in detail. For such purpose, microspectroscopy is very useful because it enables one to selectively explore the spherulite and amorphous regions of polymer blends.

In this study, four kinds of PHB/PLLA blends with the PLLA content ranging from 20 to 80 wt % have been investigated to elucidate the dispersibility and the structural details of PHB/PLLA blends. IR microspectroscopy reveals the development of spherulite structure of PHB in the PHB/PLLA blends. It is found that PHB crystallizes in any blends and that the crystalline structure of PHB in the 20/80 blend is different from those of other kinds of blends. PHB crystallizes as very small spherulites or immature spherulites under such blend ratio. The fusion peaks of DSC curve for PHB and PLLA do not shift in any blends, and the recrystallization peak for PLLA shifts to a lower temperature in the 20/80 blend. These DSC results indicate the nonisothermal crystallization rate of PLLA in the 20/80 blend is larger than that of pure PLLA.

Experiment

Preparation of Blends. PHB and PLLA were obtained from the Proctor and Gamble Co. and Shimadzu Corp. (LACTY5000). Blends of PHB and PLLA were prepared by dissolving them together in hot chloroform and then casting the solution on an aluminum dish as a film. To evaporate the solvent completely, the films were kept at 60 °C in a vacuum-dried oven for 12 h and cooled to room temperature. For the measurements of polarized light microscopy and FT-IR microspectroscopy, the blend films were pretreated by using a Mettler-Toledo FP82HT hot stage. The blend films were heated to 190 °C, kept at this temperature for 3 min, and then cooled to 60 °C. The films were kept at this temperature for 12 h, and finally, they were cooled to room temperature. The blending ratios of PHB/PLLA were 20/80, 40/60, 60/40, and 80/20 by weight. Thicknesses of the blend films were 150−200 μm.

Polarized Light Microscopy. Polarized light microscopy images were obtained with an Olympus BX51 polarizing optical microscope attached with a Smith Detection IlluminatIR FT-IR microspectrometer. The cross-polarized images of samples were viewed with transmitted light (diascopic) illumination. Visible light was focused on the surface of films of PHB, PLLA, and their blends so that we could obtain polarized light microscopy images from the surface.

FT-IR Microspectroscopy. The IR spectra were measured with the above FT-IR microspectrometer equipped with a mercury cadmium telluride (MCT) detector. Micro-IR spectra were collected at a 4 cm^{-1} spectral resolution by attenuated total reflection (ATR) mode, and 512 scans were coadded. The ATR element used was made of type II diamond (refractive index is 2.42) with the incident angle of 45°. The spatial resolution was 12 μm diameter.

IR transmission spectra were measured with a Thermo electron Nexus 470 spectrometer equipped with a MCT detector. They were collected at a 4 cm^{-1} spectral resolution, and 64 scans were coadded. The temperature of sample was controlled by using a temperature controller unit (model LT230, CHINO). The blend samples for the IR measurement were prepared by casting their chloroform solutions on CaF_2 plates.

Differential Scanning Calorimetry (DSC). DSC measurements were performed on a Perkin-Elmer Pyris6 DSC system over a temperature range from 20 to 200 °C at heating and cooling rates of 2 °C /min. The analysis of DSC curves for both the heating and cooling processes was carried out for the second run data.

Chemometrics. The Sirius software (Pattern Recognition Systems, Bergen, Norway) was employed for the quantitative

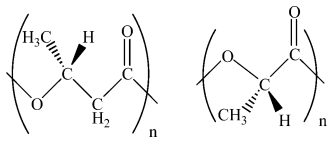

Figure 1. Chemical structures of PHB and PLLA.

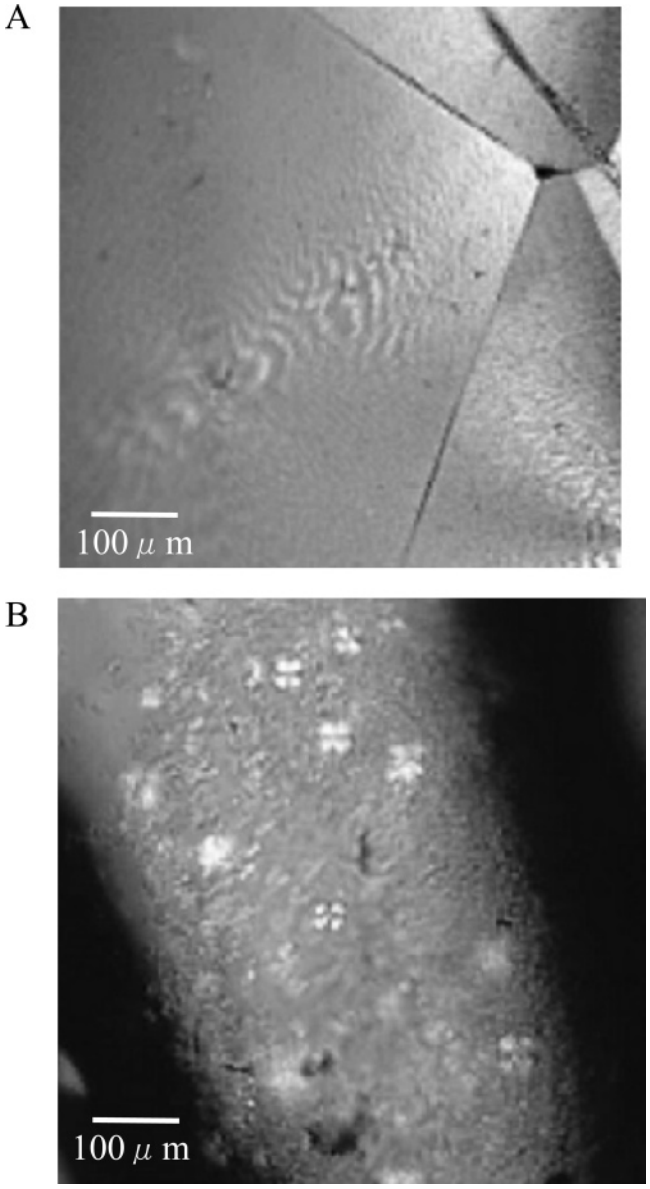

Figure 2. Polarized light microscopy images of cast films of PHB and PLLA at room temperature: (A) PHB, (B) PLLA.

estimation of the PHB content in the PHB/PLA blends. A calibration model for the estimation of the PHB content was developed by use of partial least-squares regression (PLSR). The spectra in the C=O stretching vibration region (1850−1650 cm^{-1}) were used for the chemometrics analysis.

Results and Discussion

Micro IR Spectra of PHB and PLLA and IR Spectra of Their Crystalline and Premelt States. Parts A and B of Figure 2 respectively show polarized light microscopy images of PHB and PLLA films at room temperature. The penetration depth for the ATR measurements in the present conditions was ca. 2 μm at 1000 cm^{-1} where the penetration depth is deepest. In our previous study, we compared ATR spectra of a PHB film with its transmission spectra and found that the surface region of the film sample contains more crystalline parts than its inside.[46] However, the molecular structure of PHB in the crystalline parts should not change between the surface region with 1−2 μm depth and the inside.

Parts A and A′ of Figure 3′ respectively show micro-ATR/IR spectra in the regions of 1850−1650 and 1500−1000 cm^{-1} of PHB. Parts B and B′ of Figure 3′ depict those of PLLA. Table 1 summarizes band assignments of the IR spectra of PHB and PLLA based on refs 38, 39, 41, and 43. The assignments of PHB are also compared to those of PLLA because the chemical structure of PHB is similar to that of PLLA. The spectra of two different positions (one is a small spot with a diameter of 10 μm that looks black and another is the center of spherulite structure, position 1 and 2, respectively) of a PHB film yield very similar peak intensities and frequencies in the C=O stretching band region (1800−1700 cm^{-1}) and the C−O−C and C−C stretching and CH deformation band region (1300−1000 cm^{-1} region). Both spectra have the similar appearance typical of PHB crystalline spectrum. We investigated the C=O stretching bands of the crystalline and amorphous parts of PHB by measuring temperature-dependent IR spectra of PHB.[41] It was found that PHB shows two major C=O stretching bands at 1740 and 1723 cm^{-1} due respectively to the amorphous and crystalline states. Thus, the observations in Figure 3A suggest that both positions consist largely of crystalline structure with minor amorphous component.

Spectra of PLLA samples show double peaks at 1752 and 1744 cm^{-1} due to the C=O stretching modes (Figure 3B,B′). The higher frequency band is stronger in the spectrum of a position that is the center of spherulite structure (position 1), while the lower one is more intense in the spectrum of another position where spherulite structures are not observed (position 2). We observed in the isothermal crystallization study of PLLA at 220 °C that the intensity of the higher frequency band increases, whereas that of the lower one decreases, during the crystallization process.[44] The present result is in a good agreement with the result obtained for the isothermal crystallization study. It is noted that a band at 1265 cm^{-1} due to the C−O−C stretching and CH deformation coupling mode of position 1 of PLLA is weaker than the corresponding band of the spectrum of position 2, while bands at 1179 and 1125 cm^{-1} due to the C−O−C stretching and CH_3 rocking modes of position 1 are stronger than the corresponding bands of the position 2. Therefore, it is concluded that the micro-IR spectrum of position 1 reflects the highly crystallized parts of PLLA, while that of position 2 is due to the much less crystallized part of PLLA. In fact, because of the higher T_g (59 °C) of PLLA, the overall crystallinity of the solution-casted film of PLLA prepared at 60 °C is very much lower that of PHB, which has low T_g (−6 °C). Our polarized light microscopy and micro-IR spectra clearly show that the perfect and homogeneous spherulite structure is formed in the PHB film, while less ordering and inhomogeneous structures exist in the PLLA film. To investigate the observed spectral differences between two positions in PHB and PLLA, we measured IR spectra for the premelt and crystalline states of PLLA and PHB.

Figure 4 shows the IR transmittance spectra of the premelt and crystalline states of PHB and PLLA. The

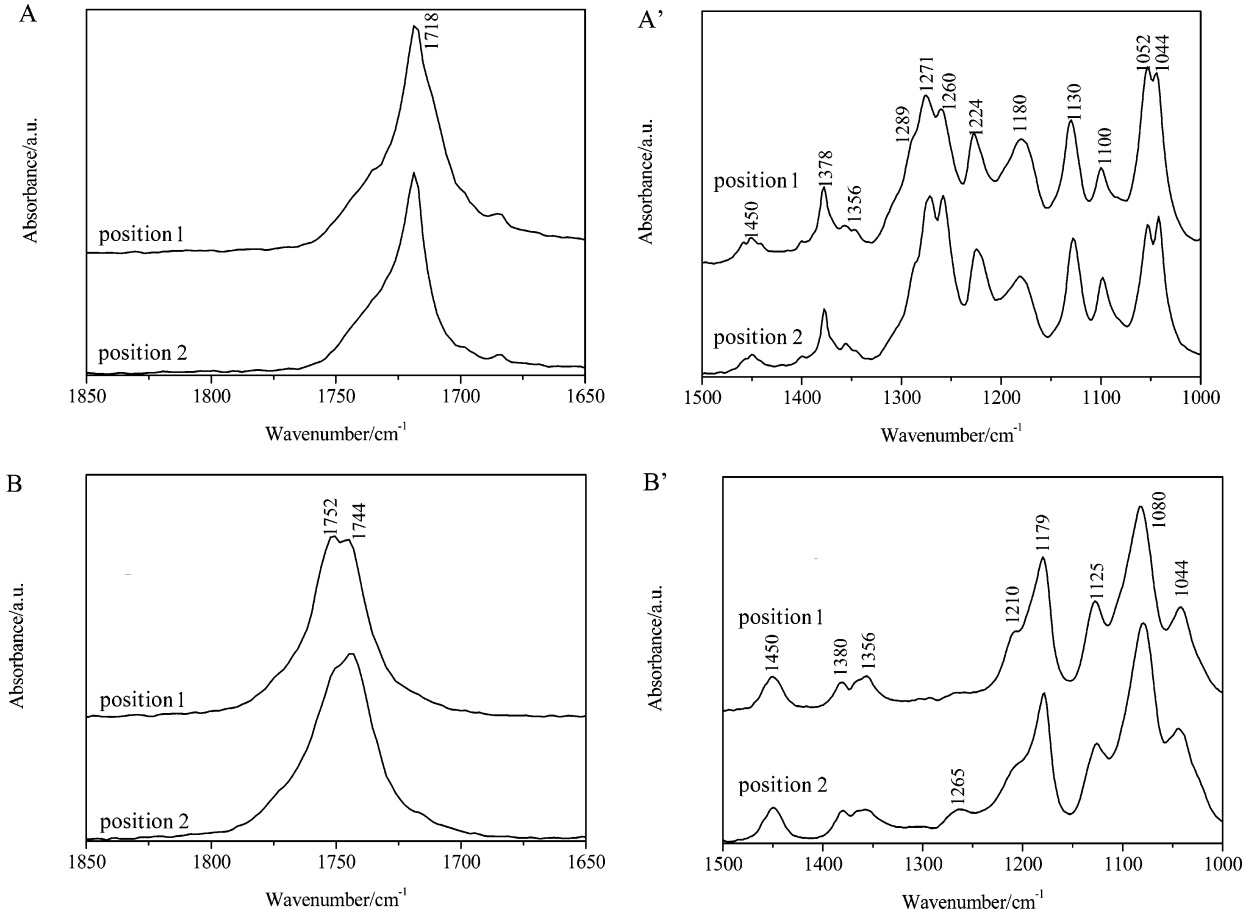

Figure 3. Micro-IR spectra of two different positions of PHB and PLLA: (A) PHB (1850−1650 cm^{-1}), (A′) PHB (1500−1000 cm^{-1}), (B) PLLA (1850−1650 cm^{-1}), (B′) PLLA (1500−1000 cm^{-1}).

Table 1. Wavenumbers (cm^{-1}) and Assignments of the IR Bands of PHB and PLLA[a]

	PHB	PLLA
1752		C=O stretching (C)
1747	C=O stretching (A)	
1744		C=O stretching (A)
1718	C=O stretching (C)	
1450	CH_3 asymmetric deformation	CH_3 asymmetric deformation
1380	CH_3 symmetric deformation	CH_3 symmetric deformation
1356	CH deformation and CH_3 symmetric deformation	CH deformation and CH_3 symmetric deformation (C)
1289	CH deformation (C)	
1276	C−O−C stretching (C)	
1271	C−O−C stretching (A)	
1265		C−O−C stretching + CH deformation (A)
1260	C−O−C stretching + CH deformation (C)	
1258	C−O−C stretching + CH deformation	
1227	C−O−C stretching (C)	
1224	C−O−C stretching (A)	
1210		C−O−C stretching (C)
1179	C−O−C stretching	C−O−C stretching
1130	CH_3 rocking	
1125		CH_3 rocking
1100	C−O−C stretching	
1080		C−O−C stretching
1054	C−O stretching	
1044	C−CH_3 stretching	C−CH_3 stretching

[a] A = amorphous; C = crystalline.

IR spectra of the premelt and crystalline states were collected at 173 °C and room temperature for PHB and at 170 °C and room temperature for PLLA. The PHB and PLLA samples at room temperature were prepared by cooling the corresponding melt samples gradually from 190 °C. Since the premelt states of PHB and PLLA consist largely of the amorphous components, the micro-IR spectra of mostly amorphous regions of PHB and PLLA may be compared with the corresponding premelt spectra. On the other hand, the annealed samples are largely composed of crystalline spherulites; thus, the micro-IR spectra of spherulite structure may be compared with the spectra of the annealed samples. Comparison between the spectra in Figures 3 and 4 reveals that it is difficult to measure the spectrum of an amorphous part of the PHB film because of its high crystallinity. However, the difference observed between the spectra of two different positions of PLLA (Figure 3B,B′) is similar to those between the spectra of the premelt and crystalline states (Figure 4B,B′).

Macro-IR Spectra of PHB/PLLA Blends. Figure 5 depicts polarized light microscopy images of the four kinds of PHB/PLLA blends. The large spherulite structures are observed for the 80/20, 60/40, and 40/60 blends. However, the polarized light microscopy image of the 20/80 blend is quite different from those of other blends. Noda et al.[45] observed that the particle size of PHA in PLLA tends to be small if the PHBHx content is small (i.e.,<20%), and it can become below 2 μm. Under such particle size, the rate of crystallization becomes very slow for PHA due to the size effect. Discernible spherulite structure of PLLA is not found in any of the PHB/PLLA blends investigated. This result indicates that PLLA exists as amorphous or very tiny

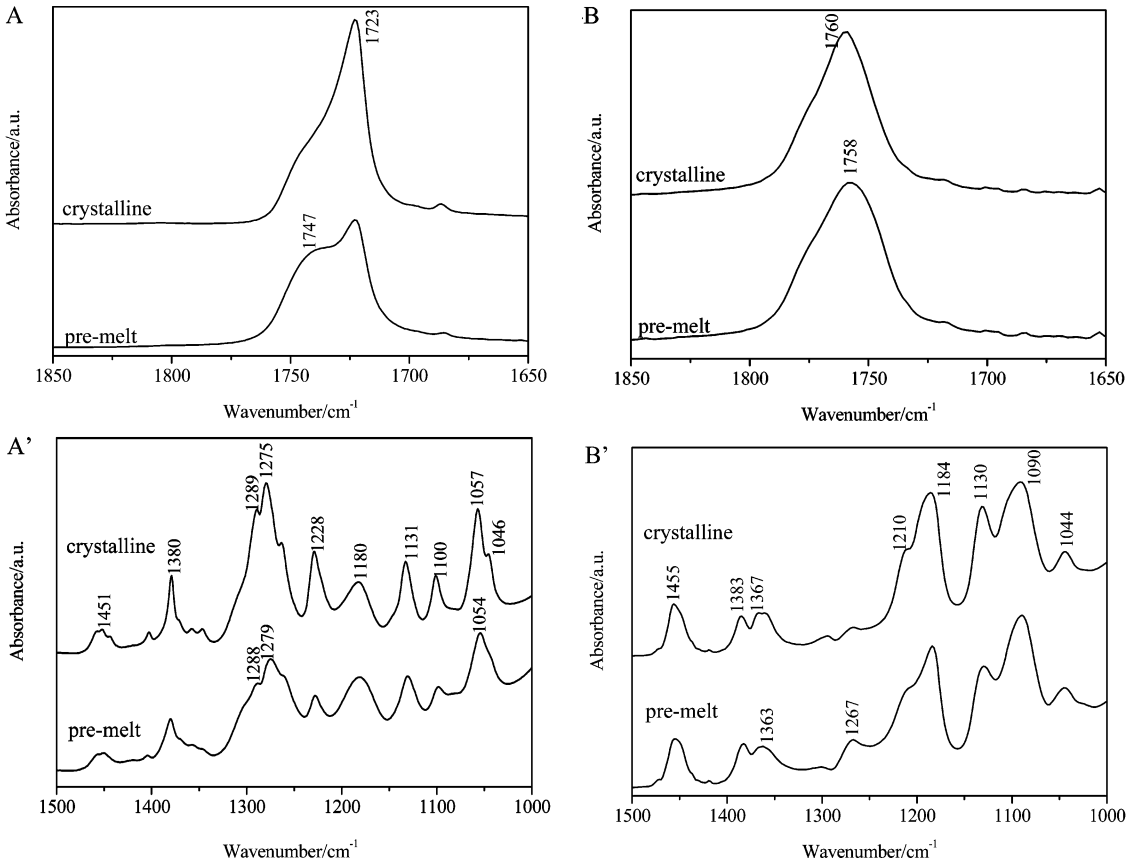

Figure 4. IR spectra of premelt and crystalline states of PHB and PLLA: (A) PHB (1850−1650 cm^{-1}), (A′) PHB (1500−1000 cm^{-1}), (B) PLLA (1850−1650 cm^{-1}), (B′) PLLA (1500−1000 cm^{-1}).

and immature spherulite structures.[32] Too tiny spherulite structures are not observed by polarized light microscopy due to insufficient spatial resolution.

Figure 6 shows IR spectra of the 80/20, 60/40, 40/60, and 20/80 blends. These spectra are also collected with the ATR mode. The measurement spot size for these spectra was 1.5 mm, and thus, these spectra are macro-IR spectra. As can be seen in Figure 6, the intensity ratio of two major C=O stretching bands at 1752 and 1718 cm^{-1} due to PLLA and PHB, respectively, changes with the blending ratio. Therefore, each blend sample contains each component corresponding to the blending ratio.

Micro-IR Spectra of PHB/PLLA Blends. Figure 7 shows micro-IR spectra of the 80/20, 60/40, 40/60, and 20/80 blends. For the comparison of spectra, the IR spectra of the blends and those of pure components (PHB or PLLA) are shown by solid and broken lines, respectively. The IR spectra of positions, where spherulite structures are observed (position 1), of the 80/20, 60/40, and 40/60 blends are very similar to that of PHB. The C=O stretching band of such positions appears at 1718 cm^{-1}, and that of other positions, where are not observed spherulite structures (position 2), appears at 1718, 1744, and 1755 cm^{-1}. The latter two bands are assigned respectively to the amorphous and crystalline bands of PLLA.[44] Bands in the C−O−C and C−C stretching and the CH deformation mode region (1300−1000 cm^{-1}) of position 1, of the 80/20, 60/40, and 40/60 blends are observed at almost the same wavenumbers as those of pure PHB. Thus, it seems that only the mostly amorphous region of the blend sample includes PLLA component. It is also noted that there is no peak shift in the IR spectra between the spherulite of the blends and of pure PHB. Table 2 summarizes the wavenumbers and assignments of IR bands observed for two different positions of the 40/60 blend, where spherulite structures are observed (position 1) and those are not observed (position 2). The wavenumbers and assignments for the 80/20, 60/40, and 20/80 blends are almost identical with those of the 40/60 blend. Peak shifts are not observed for either PHB or PLLA bands in all the blends investigated. These results indicate that PHB and PLLA are most likely immiscible in the blends and that there are no strong molecular interactions between PHB and PLLA. This observation supports the view that the spherulite structures observed in the polarized light microscopy images are due to PHB.

The IR spectra of (position 2) in the blends contain contributions from both PHB and PLLA. The percentages of the contributions from PHB and PLLA depend on the blending ratio. For the 80/20 blend, although the PHB content is high, the spectrum of such positions include substantial contribution by bands due to PLLA (Figure 7A). The C=O stretching bands of such positions of the 80/20 blend appear at 1718, 1744, and 1755 cm^{-1}. The appearance of the band at 1718 cm^{-1} indicates that such positions contain a small contribution from crystalline PHB. The latter two bands are assigned to the amorphous and crystalline bands of PLLA, and one of the C−O−C stretching bands of PLLA is identified at 1084 cm^{-1}.

For the 20/80 blend, which did not have the observable PHB spherulites, we show two spectra obtained from different positions (position 1 and 2) (Figure 7D,D′). Note that both spectra show the C=O stretching bands at 1718, 1744, and 1755 cm^{-1}, although the relative intensities of the three bands are quite different

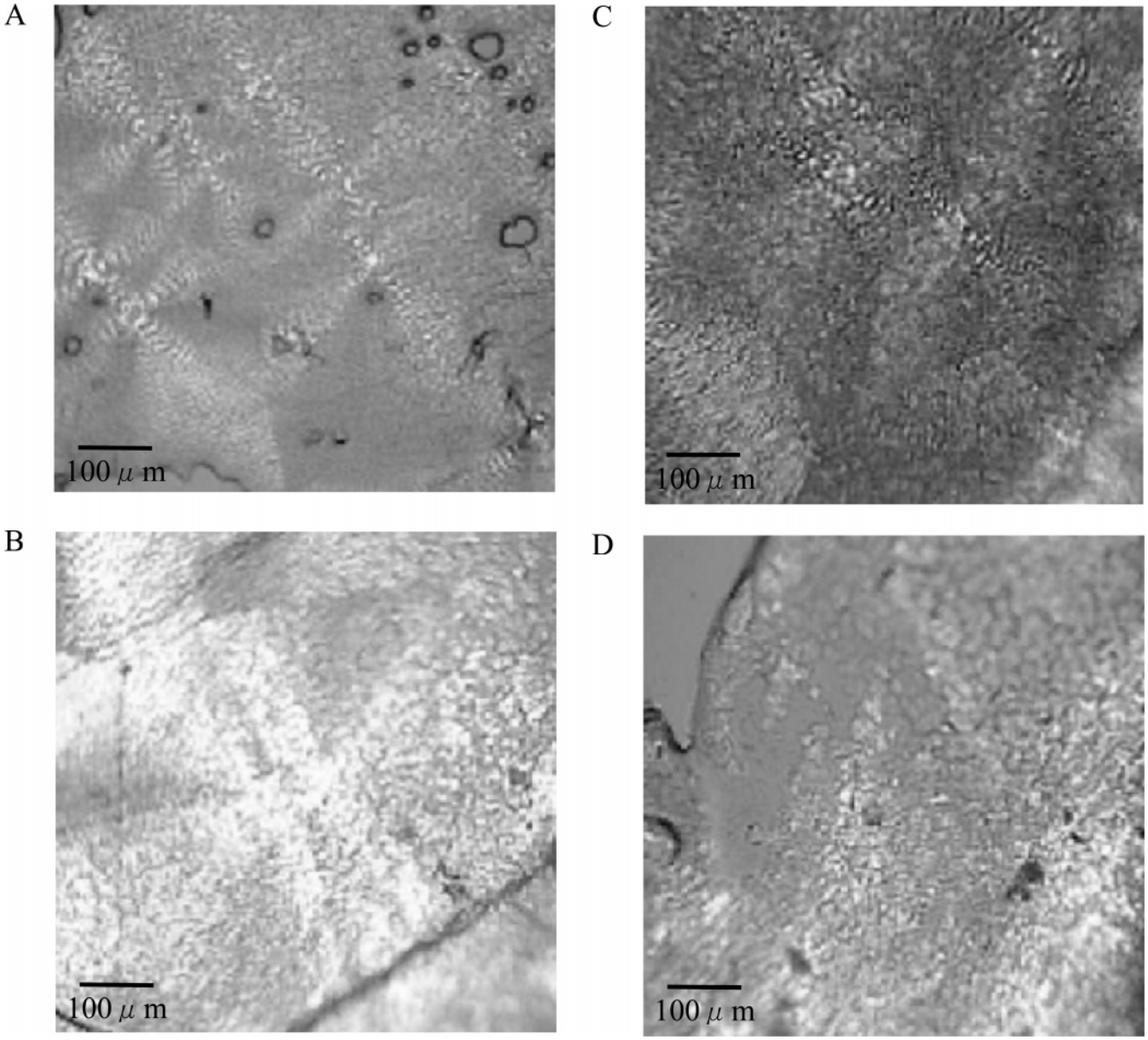

Figure 5. Polarized light microscopy images of cast films of PHB/PLLA blends: (A) PHB/PLLA = 80/20, (B) PHB/PLLA = 60/40, (C) PHB/PLLA = 40/60, (D) PHB/PLLA = 20/80.

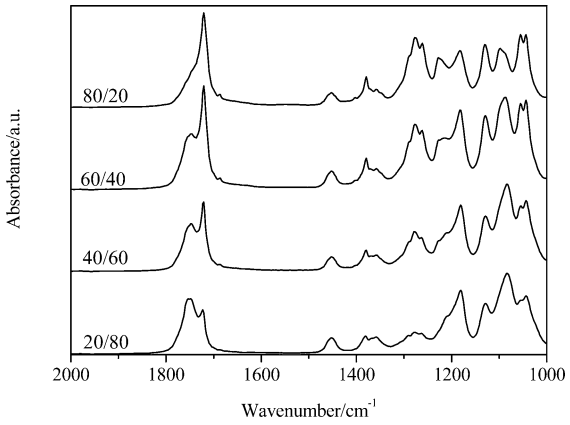

Figure 6. Macro-IR spectra of PHB/PLLA blends.

between the two spectra. Micro-IR spectra measured in some spots are similar to the pure PLLA spectrum. Such spectra also have a C=O stretching band at 1718 cm^{-1} ascribed to crystalline PHB. It means that the small crystalline structure of PHB still exists in the 20/80 blend although no observable spherulite crystal can be found under polarized light microscopy. They show the C−O−C stretching band of PHB at 1224 cm^{-1} and that of PLLA at 1082 cm^{-1} (Figure 7D′). From these results, we conclude that the 20/80 blend also has an inhomogeneous structure.

Prediction of PHB Contents in the Blends by Chemometrics. Figure 8 shows a PLSR calibration model for the prediction of the PHB content in the PHB/PLLA blends. The PLSR calibration model was developed by use of the macro-IR spectra in the C=O stretching region of the blends shown in Figure 6 to predict the PHB content (%) in the blends. The regression coefficient (R) and the standard error of prediction (SEP) of the PLSR model were 0.9908 and 5.84, respectively. After the development of the calibration model, the micro-IR spectra were adapted to the calibration model to predict the contents of PHB. The estimated PHB ratios and their deviations are listed in Table 3. As can be seen in Table 3, the estimated PHB contents in positions, where spherulite structures are observed

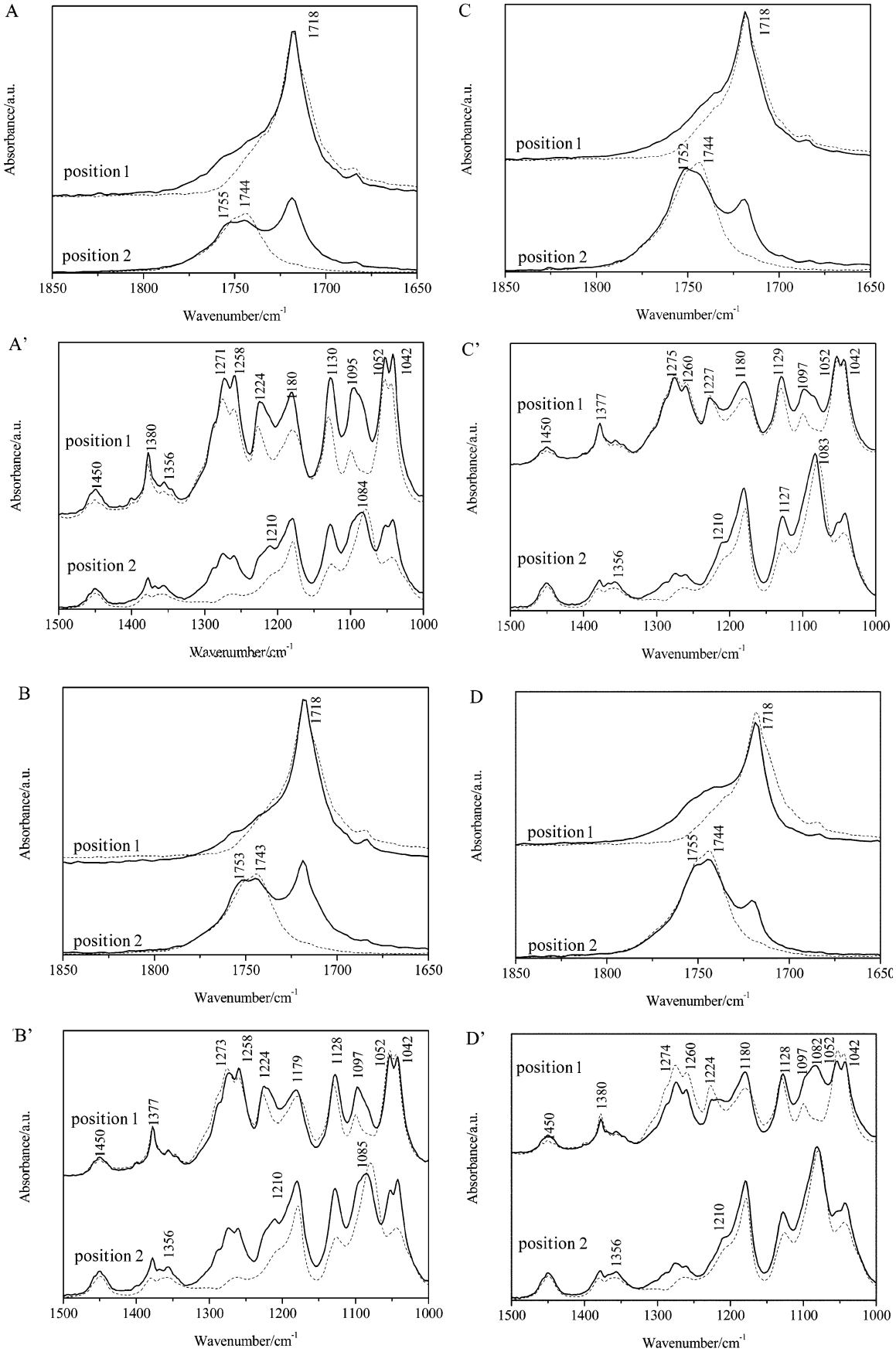

Figure 7. (A, B, and C) Micro-IR spectra of two different positions of PHB/PLLA blends: (A) PHB/PLLA = 80/20 (1850−1650 cm^{-1}), (A′) PHB/PLLA = 80/20 (1500−1000 cm^{-1}); (B) PHB/PLLA = 60/40 (1850−1650 cm^{-1}), (B′) PHB/PLLA = 60/40 (1500−1000 cm^{-1}); (C) PHB/PLLA = 40/60 (1850−1650 cm^{-1}), (C′) PHB/PLLA = 40/60 (1500−1000 cm^{-1}). (D) Micro-IR spectra of two amorphous parts of PHB/PLLA 20/80 blend: (D) PHB/PLLA = 20/80 (1850−1650 cm^{-1}), (D′) PHB/PLLA = 20/80 (1500−1000 cm^{-1}).

Table 2. Wavenumbers (cm^{-1}) and Assignments of the IR Bands of PHB/PLLA = 40/60 Blends[a]

	position 1	position 2
1752		C=O stretching (PLLA, C)
1744		C=O stretching (PLLA, A)
1718	C=O stretching (PHB,C)	C=O stretching (PHB, C)
1450	CH_3 asymmetric deformation (PHB)	CH_3 asymmetric deformation (PLLA)
1377	CH_3 symmetric deformation (PHB)	CH_3 symmetric deformation (PHB)
1356	CH deformation and CH_3 symmetric deformation	CH deformation and CH_3 symmetric deformation
1275	C−O−C stretching (PHB, C)	C−O−C stretching (PHB)
1260	CH deformation + C−O−C stretching (PHB)	CH deformation + C−O−C stretching (PHB)
1227	C−O−C stretching (PHB, C)	
1180	C−O−C stretching (PHB)	C−O−C stretching
1129	CH_3 rocking (PHB)	
1127		CH_3 rocking (PLLA)
1097	C−O−C stretching (PHB)	
1083		C−O−C stretching (PLLA)
1052	C−O stretching (PHB)	
1042	C−CH_3 stretching (PHB)	C−CH_3 stretching (PLLA)

[a] A = amorphous; C = crystalline.

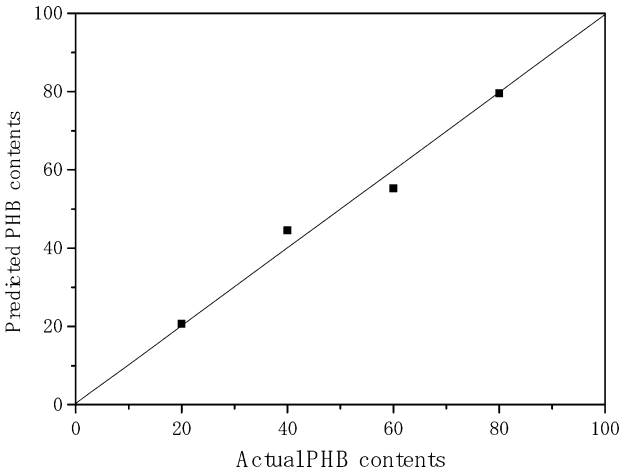

Figure 8. A PLSR calibration model for the prediction of the PHB ratio in PHB/PLLA blends.

Table 3. Predicted Contents of PHB in Two Different Positions of PHB/PLLA Blends Estimated by a PLSR Calibration Model and Their Standard Deviation

		predicted PHB content (%)	standard deviation (%)
80/20 blend	position 1	93.749	8.716
	position 2	48.208	8.208
60/40 blend	position 1	104.836	9.124
	position 2	44.227	8.375
40/60 blend	position 1	97.900	8.326
	position 2	8.922	8.369
20/80 blend	position 1	67.233	8.311
	position 2	3.516	8.360

(position 1), of 80/20, 60/40, and 40/60 blends are nearly 100%. However, those in other positions (position 2) of these blends are lower than the actual blending ratio. For the 20/80 blend, the estimated contents change with measurement spots. Some of the estimated contents are higher than the actual blending ratio, but some others are lower than that. These results show that PLLA is localized in the positions where the spherulite structures are not observed in each blend.

DSC. The samples employed for DSC analysis were the same films as used for the polarized light microscopy observations. Figure 9A,B displays the cooling and heating processes observed in the DSC scans during the cooling and heating of PHB, PLLA, and their blends. For the cooling processes of PHB and PLLA (Figure 9A), the crystallization peak of PHB appears at 107 °C, while that of PLLA does not appear clearly. From this result, one can conclude that the crystallinity of PHB is higher than that of PLLA. The crystallization peak of PHB is observed for the 80/20 and 60/40 blends, but the corresponding peak is not observed for the 40/60 and 20/80 blends. This indicates that PHB in the latter two blends did not crystallize much during the DSC cooling process. However, the polarized light microscopy images and micro-IR spectra of the 40/60 blend clearly detect the spherulite structure of PHB. The spherulite structure of the 40/60 blend may be generated in the holding process at 60 °C for 12 h. In Figure 10, the heat of crystallization, as characterized by the DSC peak areas in the curves of the cooling process, are plotted as a function of PLLA content for the blends. The heat of crystallization of PHB change with the blending ratio.

For the heating processes (Figure 9B), on the other hand, the fusion peak of PHB appears clearly at 173 °C as double peaks and that of PLLA appears at 173 °C as a single peak. There are two possibilities for the origin of the two peaks in the heating cycle of DSC.[47] One is the melting and subsequent recrystallization of PHB. The other possibility is that there are two types of lamellae structures in the crystal. The fusion double peaks of PHB are also observed for the 80/20, 60/40, and 40/60 blends, but the corresponding double-peak feature is not observed for the 20/80 blend. Since the fusion peaks of PHB and PLLA are located almost at the same temperature, it is difficult for the fusion peaks of the blends to be distinguished into each component peak. In this study, there is no change in the melting point of PHB. Therefore, the double-peak feature of PHB thermogram may correspond to the melting and recrystallization of PHB. The recrystallization peak of pure PLLA appears at 107 °C. Only the 20/80 blend has a similar peak at 88 °C. This means that only the 20/80 blend can recrystallize PLLA component and that the recrystallization temperature of PLLA in the 20/80 blend is much lower than that of pure PLLA. The lowering of recrystallization temperature suggests that the nonisothermal crystallization rate of PLLA in the 20/80 blend is faster than that of pure PLLA. It is reasonable to speculate that PHB forms small finely dispersed crystals during the cooling process, which may act as nucleation sites of PLLA. Thus, the nonisothermal crystallization rate of PLLA in the 20/80 blend becomes faster than that of pure PLLA in the subsequent heating processes. On the other hand, PLLA is not crystallized faster in other blends because PHB forms large spherulitic crystals that do not act as efficient nucleation sites for PLLA.

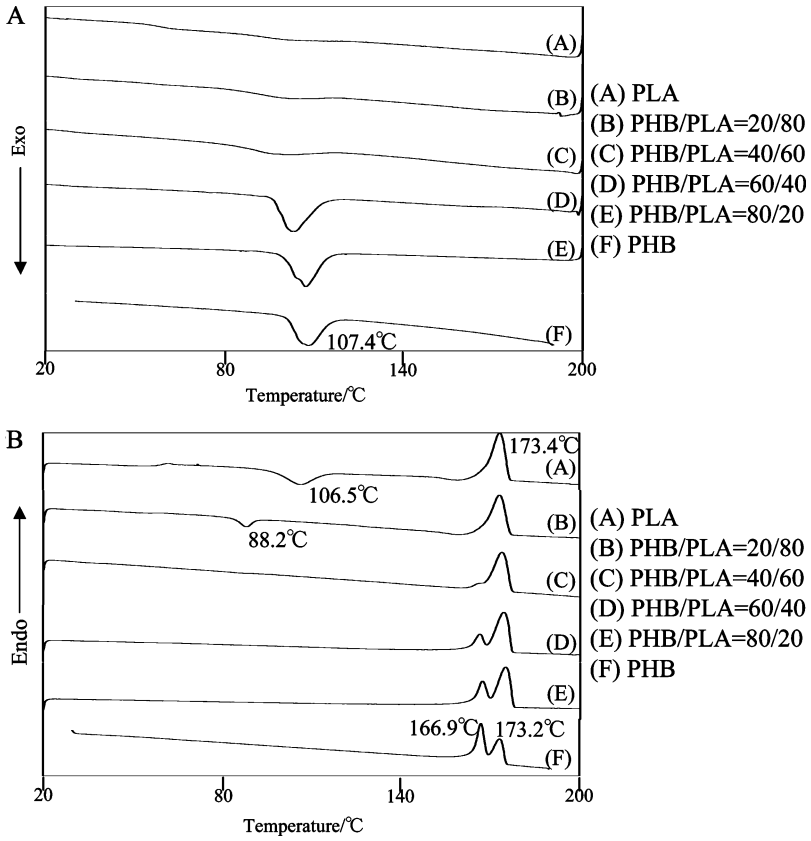

Figure 9. DSC scans during the cooling and heating processes of PHB, PLLA, and the four kinds of PHB/PLLA blends: (A) cooling process, (B) heating process.

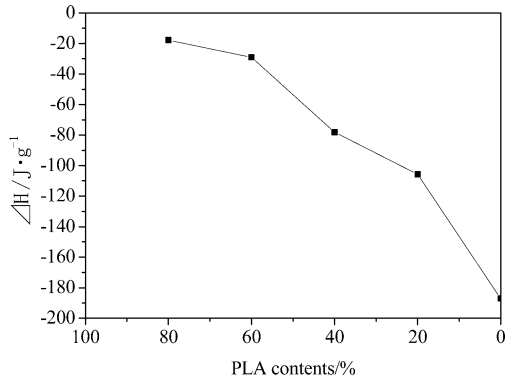

Figure 10. Heats of crystallization of PHB vs the PLLA content for the PHB/PLLA blends.

Conclusion

This study has investigated the structure, dispersibility, morphology, and crystallinity of PHB/PLLA blends by using FT-IR microspectroscopy and DSC. The following conclusions can be reached from the present study. Spatially resolved micro-IR spectra selectively characterizing the spherulite and predominantly amorphous region in PHB/PLLA blends can be obtained. The spectra in a position, where spherulite structure is observed, of 80/20, 60/40, and 40/60 blends are very similar to that of crystallized PHB; thus, the present IR study has revealed the crystallization of PHB in these blends. The spectra in another position, where spherulite structure is not observed, of these blends contain both PHB and PLLA bands, and peak intensities of each component change with the blending ratio. In the case of 20/80 blend, which did not show the development of observable spherulites, the micro-IR spectra measured at any positions include contributions from both PHB and PLLA. The peak intensity ratio of PHB and PLLA bands varies largely with measurement position in this blend. These micro-IR results indicate all the PHB/PLLA blends have inhomogeneous structures. The crystalline peak area of DSC of PLLA changes with the blending ratio. The fusion peaks can be detected for PHB and PLLA. However, the peaks of PHB and PLLA are observed at almost the same temperatures, so that it is difficult to estimate the heat of fusion for each component separately. The recrystallization peak of PLLA can be detected in the 20/80 blend, and the lowering of the recrystallization temperature in the blend suggests that PHB forms some small crystals that act as the nucleation of PLLA.

It has been confirmed by micro-IR spectroscopy and DSC that the investigated blends of PHB/PLLA are immiscible. The spherulite structure of PHB was observed in the blends by FT-IR microspectroscopy. The crystallization and fusion temperatures of PHB and PLLA are constant in all the blends. These results also support the immiscibility of PHB/PLLA blends. Meanwhile, it has been found that the growth of spherulite of PHB is confined in this 20/80 blend.

References and Notes

(1) Doi, Y., Steinbuchel, A., Eds.; *Biopolymers, Polyesters I–III*; Wiley: New York, 2001; Vols. 3, 3b, and 4.
(2) Doi, Y. *Microbial Polyesters;* VCH Publishers: NewYork, 1990.
(3) Anderson, A. J.; Dawes, E. A. *Microbiol. Rev.* **1990**, *54*, 450.
(4) Lundgren, D. G.; Alper, R.; Schnaitman, C.; Marchessault, R. H. *J. Bacteriol.* **1965**, *89*, 245.
(5) Dawes, E. A. *Novel Biodegradable Microbial Polymers*; Kluwer: Dordrecht, 1990.

(6) Lara, L. M.; Gjalt, W. H. *Microbiol. Mol. Biol. Rev.* **1991**, *63*, 21.
(7) Satkowski, M. M.; Melik, D. H.; Autran, J. P.; Green, P. R.; Noda, I.; Schechtman, L. A. In *Biopolymers;* Steinbuchel, A., Doi, Y., Eds.; Wiley-VCH: Wienheim, 2001; p 231.
(8) Iwata, T.; Doi, Y. *Macromol. Chem. Phys.* **1999**, *200*, 2429.
(9) Yoshie, N.; Menju, H.; Sato, H.; Inoue, Y. *Macromolecules* **1995**, *28*, 6516.
(10) Doi, Y.; Kitamura, S.; Abe, H. *Macromolecules* **1995**, *28*, 4822.
(11) Abe, H.; Doi, Y.; Aoki, H.; Akehata, T. *Macromolecules* **1998**, *31*, 1791.
(12) Yoshie, N.; Saito, M.; Inoue, Y. *Macromolecules* **2001**, *34*, 8953.
(13) Avella, M.; Martuscelli, E. *Polymer* **1988**, *29*, 1731.
(14) Greco, P.; Martuscelli, E. *Polymer* **1989**, *30*, 1475.
(15) Azuma, Y.; Yoshie, N.; Sakurai, M.; Inoue, Y.; Chujo, R. *Polymer* **1992**, *33*, 4763.
(16) Gassner, F.; Owen, A. J. *Polymer* **1994**, *35*, 2233.
(17) Dorgan, J. R. *Poly(lactic acid) Properties and Prospects of an Environmentally Benign Plastic*; American Chemical Society: Washington, DC, 1999; p 145.
(18) Ikada, Y.; Tsuji, H. *Macromol. Rapid Commun.* **2000**, *21*, 117.
(19) Urayama, H.; Kanamori, T.; Kimura, Y. *Macromol. Mater. Eng.* **2002**, *287*, 116.
(20) Penning, J. P.; Dijkstra, H.; Pennings, A. J. *Polymer* **1993**, *34*, 942.
(21) Schakenraad, J. M.; Oosterbaan, J. A.; Nieuwenhuis, P.; Molenaar, I.; Olijslager, J.; Potman, W.; Eenink, M. J. D.; Feijen, J. *Biomaterials* **1988**, *9*, 116.
(22) Jackanicz, T. M.; Nash, H. A.; Wise, D. L.; Gregory, J. B. *Contraception* **1973**, *8*, 227.
(23) Leenslag, J. W.; Pennings, A. J.; Bos, R. R. M.; Rozema, F. R.; Boering, G. *Biomaterials* **1987**, *8*, 311.
(24) Hu, Y.; Hu, Y. S.; Topolkaraev, V.; Hiltner, A.; Baer, E. *Polymer* **2003**, *44*, 5681.
(25) Hu, Y.; Rogunova, M.; Topolkaraev, V.; Hiltner, A.; Baer, E. *Polymer* **2003**, *44*, 5701.
(26) Hu, Y.; Hu, Y. S.; Topolkaraev, V.; Hiltner, A.; Baer, E. *Polymer* **2003**, *44*, 5711.
(27) Ke, T.; Sun, X. *J. Appl. Polym. Sci.* **2003**, *89*, 1203.
(28) Wang, H.; Sun, X.; Seib, P. *J. Appl. Polym. Sci.* **2003**, *90*, 3683.
(29) Gazzano, M.; Focarete, M. L.; Riekel, C.; Scandola, M. *Biomacromolecules* **2004**, *5*, 553.
(30) Ohkoshi, I.; Abe, H.; Doi, Y. *Polymer* **2000**, *41*, 5985.
(31) Blümm, E.; Owen, A. J. *Polymer* **1995**, *36*, 4077.
(32) Zhang, L.; Xiong, C.; Deng, X. *Polymer* **1996**, *37*, 235.
(33) Abe, H.; Doi, Y.; Aoki, H.; Akehata, T. *Maclomolecules* **1998**, *31*, 1791.
(34) Xu, J.; Guo, B. H.; Yang, R.; Wu, Q.; Chen, G. Q.; Zhang, Z. M. *Polymer* **2002**, *43*, 6893.
(35) Yoshie, N.; Asaka, A.; Yazawa, K.; Kuroda, Y.; Inoue, Y. *Polymer* **2003**, *44*, 7405.
(36) Zhang, J.; Tsuji, H.; Noda, I.; Ozaki, Y. *J. Phys. Chem. B* **2004**, *108*, 11514.
(37) Kang, S.; Hsu, S. L.; Stidham, H. D.; Smith, P. B.; Leugers, M. A.; Yang, X. *Macromolecules* **2001**, *34*, 4542.
(38) Kister, G.; Cassanas, G.; Vert, M. *Polymer* **1998**, *39*, 267.
(39) Kister, G.; Cassanas, G.; Vert, M.; Pauvert, B.; Terol, A. *J. Raman Spectrosc.* **1995**, *26*, 307.
(40) Sawai, D.; Takahashi, K.; Sasashige, A.; Kanamoto, T.; Hyon, S. H. *Macromolecules* **2003**, *36*, 3601.
(41) Sato, H.; Murakami, R.; Padermshoke, A.; Hirose, F.; Senda, K.; Noda, I.; Ozaki, Y. *Macromolecules* **2004**, *37*, 7203.
(42) Sato, H.; Nakamura, M.; Padermshoke, A.; Yamaguchi, H.; Terauchi, H.; Ekgasit, S.; Noda, I.; Ozaki, Y. *Macromolecules* **2004**, *37*, 3763.
(43) Zhang, J.; Tsuji, H.; Noda, I.; Ozaki, Y. *Macromolecules* **2004**, *37*, 6433.
(44) Zhang, J.; Sato, H.; Tsuji, H.; Noda, I.; Ozaki, Y. *J. Mol. Struct.* **2005**, *735*−*736*, 249.
(45) Noda, I.; Satkowski, M. M.; Dowery, A. E.; Marcott, C. *Macromol. Biosci.* **2005**, *735*−*736*, 249.
(46) Padermshoke, A.; Katsumoto, Y.; Sato, H.; Ekgasit, S.; Noda, I.; Ozaki, Y. *Polymer* **2004**, *45*, 6547.
(47) Sato, H.; Padermshoke, A.; Nakamura, M.; Murakami, R.; Hirose, F.; Senda, K.; Terauchi, H.; Ekgasit, S.; Noda, I.; Ozaki, Y. *Macromol. Symp.* **2005**, *220*, 123.

MA0504668